Cell. Mol. Life Sci. 66 (2009) 681 – 696
1420-682X/09/040681-16
DOI 10.1007/s00018-009-8645-1

Cellular and Molecular Life Sciences

Research Article

hShroom1 links a membrane bound protein to the actin cytoskeleton

D. E. Dye[a, †], S. Karlen[b, †], B. Rohrbach[b], O. Staub[c], L. R. Braathen[b], K. A. Eidne[d] and D. R. Coombe[a, *]

[a] School of Biomedical Sciences, Curtin University of Technology, Molecular Immunology Group, Level 5 MRF Building, Rear 50 Murray Street, Perth 6000 (Australia), Fax: +61 8 9224 0360, e-mail: d.coombe@curtin.edu.au
[b] Dermatological Clinic, Inselspital, Berne (Switzerland)
[c] Institute of Pharmacology and Toxicology, University of Lausanne (Switzerland)
[d] Western Australian Institute of Medical Research, Centre for Medical Research, The University of Western Australia, Perth (Australia)

Received 09 October 2008; received after revision 23 November 2008; accepted 09 December 2008
Online First 14 January 2009

Abstract. hShroom1 (hShrm1) is a member of the Apx/Shroom (Shrm) protein family and was identified from a yeast two-hybrid screen as a protein that interacts with the cytoplasmic domain of melanoma cell adhesion molecule (MCAM). The characteristic signature of the Shrm family is the presence of a unique domain, ASD2 (Apx/Shroom domain 2). mRNA analysis suggests that hShrm1 is expressed in brain, heart, skeletal muscle, colon, small intestine, kidney, placenta and lung tissue, as well a variety of melanoma and other cell lines. Co-immunoprecipitation and bioluminescence resonance energy transfer (BRET) experiments indicate that hShrm1 and MCAM interact *in vivo* and by immunofluorescence microscopy some co-localization of these proteins is observed. hShrm1 partly co-localises with β-actin and is found in the Triton X-100 insoluble fraction of melanoma cell extracts. We propose that hShrm1 is involved in linking MCAM to the cytoskeleton.

Keywords. Shroom, Apx, MCAM, CD146, melanoma.

Introduction

The Apx/Shroom (Shrm) family of actin-binding proteins is defined by the presence of a highly conserved motif, ASD2 (Apx/Shrm domain 2), which shows no homology with other known protein domains. Shrm family proteins also usually contain an N-terminal PDZ domain and/or a centrally located ASD1 motif (Apx/Shrm domain 1) [1, 2]. To date, eleven different members of the Shrm family have been described in *Xenopus*, mouse and humans. It appears that the Shrm protein family is highly conserved throughout evolution. Bioinformatic searches have identified Shrm-related proteins in all of the vertebrates examined and insect genomes such as that of *Drosophila melanogaster* also encode a related protein containing an ASD2 domain [1]. Such conservation suggests that this protein family has a critical role within the cell.

Until recently, a dual nomenclature was used for the Shrm family, with some proteins retaining the root "Apx" and others "Shroom". To simplify this, Hagens et al. (2006) proposed a standard nomenclature based on the name Shroom (Shrm), currently the most

† These authors contributed equally to this work.
* Corresponding author.

thoroughly studied member of the family [1]. This new nomenclature is used throughout this paper.

Although the members of the Shrm family contain regions of significant protein sequence similarility, different biological functions have been proposed for some of these proteins, but a common theme is an interaction with proteins of the cytoskeleton [1, 3]. The founding member of the Shrm family, xShrm1 (formerly Apx) was identified in 1992 as a plasma membrane protein involved in the activity of amiloride-sensitive sodium channels [4, 5]. This was followed by the identification of hShrm2 (formerly ApxL), a human gene cloned from the ocular albinism type 1 critical region on the X chromosome [6]. hShrm2 regulates pigmentation of the retinal pigment epithelium, possibly through an interaction with the microtubular network within the cell [3]

The best characterised members of the Shrm family, xShrm3 and mShrm3 (formerly Shroom), were found to be essential for neural tube morphogenesis in respectively, *Xenopus* and the mouse [7, 8], suggesting that the function of Shrm3 is evolutionarily conserved [9]. Through its role in apical constriction and apicobasal elongation of neurepithelial cells, a process involving an interaction of the ASD2 motif with filamentous (F) actin, Shrm3 was reported to facilitate the bending of cell sheets [8, 9]. The exact mechanism driving these cell shape changes is not clear, although interactions between mShrm3 and myosin II, as well as xShrm3 and γ-tubulin, have been proposed [9, 10]. hShrm4 (formerly *KIAA1202*) was first identified as a gene important in cognitive development [11] and has subsequently been found to bind a sub-fraction of cellular actin that is distinct from both stress fibres and cortical actin [2]. hShrm4, like Shrm3, is believed to regulate cell architecture via interactions with actin and myosin II [2]. In this report we characterise hShroom1 (hShrm1), which we isolated from a yeast two hybrid screen using the intracellular tail of melanoma cell surface adhesion molecule (MCAM) as bait.

MCAM belongs to the immunoglobulin (Ig) superfamily of cell adhesion molecules and was originally identified as a human melanoma associated antigen whose expression was positively correlated with melanoma thickness and metastatic potential [12]. MCAM has been described as an adhesion molecule that moderates cell-matrix interactions [13] and mediates cell-cell adhesion by binding a heterotypic ligand [14, 15]. Less is known about the intracellular domain of MCAM, although a number of studies have identified two MCAM isoforms, MCAM-long (MCAM-L) and MCAM-short (MCAM-S), which differ in their cytoplasmic tails (Fig. 1) [13, 16]. Anfosso et al. [16, 17] identified MCAM-L as the dominant transcript in cultured endothelial cells and also suggested that MCAM participates in signal transduction. In endothelial cells, engagement of MCAM-L initiated a protein tyrosine kinase-dependent signaling cascade that resulted in the tyrosine phosphorylation of a complex pattern of proteins, including focal adhesion kinase ($p125^{FAK}$) and paxillin, and propose that CD146 may act as a signaling molecule involved in actin cytoskeleton rearrangement. We demonstrate here that MCAM-L is preferentially expressed in melanoma cells. A yeast two-hybrid screen of a human brain cDNA library using the cytoplasmic tail of MCAM-L as bait identified hShrm as a putative intracellular binding partner(s). The interaction between hShrm1 and MCAM was unexpected and is the first report of an association between a Shrm family member and a cell-surface adhesion molecule. hShrm1 was found to be expressed in a range of tissues and in a variety of melanoma cell lines. Evidence for the interaction of hShrm1 and MCAM in melanoma cells was obtained by immunofluorescence microscopy, co-immunoprecipitation and bioluminescence resonance energy transfer (BRET) experiments. Moreover, data consistent with the conclusion that some hShrm1 molecules co-localise with β- and F-actin was obtained. Thus, in melanoma cells it appears that hShrm1 is involved in linking MCAM to the actin cytoskeleton. However, as the data suggest that only a proportion of the cellular pool of hShrm1 interacts with MCAM, it is likely that hShrm1 also interacts with other as-yet unidentified binding partners.

Materials and methods

Cell lines. The following cells were purchased from ATCC and maintained in culture according to ATCC recommendations: SK-Mel2, SK-Mel28 and A2058 (melanoma), HeLa (cervical carcinoma), HT1080 (fibrosarcoma), HL60 and U937 (promyelocytic leukemia), CHO-K1 (hamster ovary cells), HEK293 (human embryonic kidney cells) and COS-7 (monkey kidney cells). Primary human keratinocytes were from Invitrogen (Carlsbud, CA). The MM96L melanoma cells were kindly provided by Dr. Peter Parsons of the Queensland Institute of Medical Research, Australia. SB1 and SB2 cells are derived from a primary cutaneous melanoma and were a gift from Dr. B. Giovanella (Stehlin Foundation for Cancer Research, Houston, Texas, USA). Culture conditions for the SB1 and SB2 cells are described in Karlen and Braathen (1999). Where indicated, cells were treated with 20 μM forskolin (Sigma-Aldrich, St Louis, MO). Human umbilical vein endothelial (HUVEC) cells were iso-

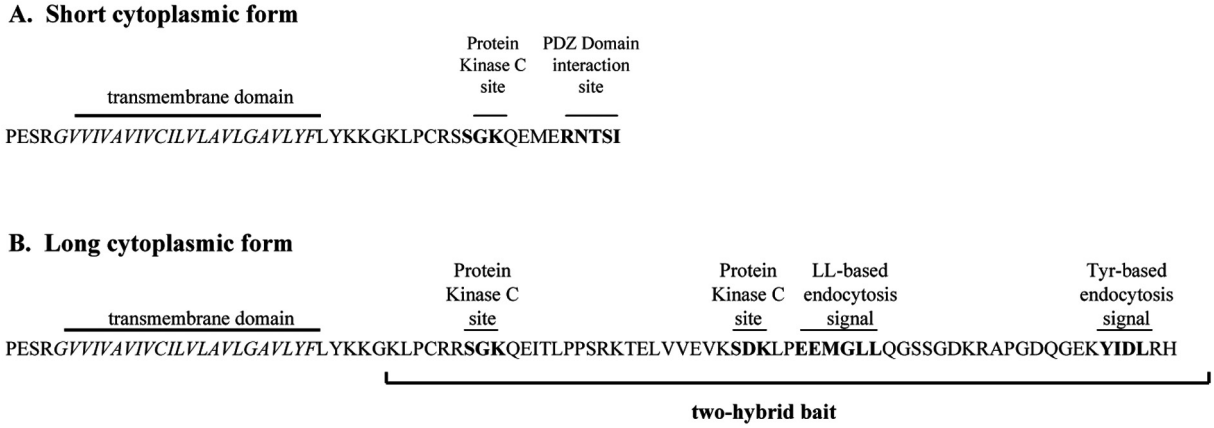

Figure 1. MCAM cytoplasmic tail variants. Amino acid sequences of the short (*A*) and long (*B*) cytoplasmic forms [13]. The putative transmembrane domain, protein kinase C (PKC) phosphorylation sites and endocytosis motifs are indicated. The region used as bait in the two-hybrid system is shown.

lated from umbilicus tissue and cultured according to the method described by Marin et al. (2001) [18].

RNA analysis. Total RNA from normal and tumor tissues were from Clontech (Palo Alto, CA). Total RNA from cell lines was prepared as described [19]. Detection of MCAM (GenBank accession no. NM_006500) and hShrm1 (GenBank accession no. AF314142) mRNA was performed using the one tube/two enzymes Access reverse transcriptase PCR system (Promega, Madison WI). Standard reactions used 100 ng of RNA. MCAM primers were: hMCAMs (nt 1346–1366) 5'-GTGTTGAATCTGTCTTGTGAA-3' and hMCAMas (nt 1930 to 1945) 5'-ATGCCTCA-GATCGATG-3'. These primers generate fragments of 600 bp and 482 bp, corresponding to the long (MCAM-L) and short (MCAM-S) MCAM cytoplasmic variants [13]. hShrm1 RNA was detected using the primers: clone7-s (nt 1675–1684) 5'-CTG TCCCAG-CTGATGCCTTG-3' and clone7-as (nt 2061–2080) 5'-CCACATGGCTGGTCAA GCAC-3'. Hybridization temperatures were 52 °C (MCAM) or 58 °C (hShrm1). PCR products were analyzed on 2% agarose gels and visualized using ethidium bromide. The human β-actin amplimer set (Clontech) was used for controls.

Constructs for the two-hybrid system. The region encoding the last 63 amino acids of MCAM was amplified by RT-PCR from SK-Mel2 total RNA. The 5' and 3' RT-PCR primers contained restriction sites (BamHI and SalI, respectively) to allow in frame insertion of MCAM with the GAL4 binding domain and the HA epitope in the vector pAS1 [20]. The resulting pAS1/MCAM construct was transfected into the yeast reporter strain Y153 cells using the lithium acetate method [21]. Western blotting of cell lysates with anti-HA antibody (Roche Diagnostics, Indianapolis, IN) indicated whether transformants expressed the GAL4-HA-MCAM fusion protein. A filter-lift β-Galactosidase assay [22] ensured that recombinant clones had not auto-activated lacZ expression.

Library screening. The screening strategy was performed as described [23]. Briefly, a colony of Y153 cells transformed with pAS1/MCAM-tail was grown in YPD-broth and transformed with a human brain cDNA library (Matchmaker, Clontech) constructed in pACT2. Transformants were selected on SD-broth plates lacking Trp, Leu and His, but containing 20 mM 3-AT (Sigma-Aldrich). Filter-lift β-Galactosidase assays were performed to select β-Galactosidase positive clones from which total DNA was isolated and transformed into HB101 cells. Transformed colonies were transferred to minimal M9 plates lacking Leu and selected for expression of LEU2 on pACT2. To check for true positives, isolated plasmids were transfected into yeast Y153 cells either alone, or with pAS1/MCAM-tail or, as negative controls, with pAS1/C-tail that encodes the cytoplasmic domain of the β-adrenergic receptor (a gift from Dr. A.L. Lattion). Liquid β-Galactosidase assays using o-nitrophenyl-β-D-galactoside (ONPG) were performed for quantitation [24]. The results were expressed as defined units [25]. Positive clones were sequenced and compared to data base entries using a Blast algorithm. A partial cDNA clone (2H-clone7) encoding the C-terminal domain of a yet unidentified protein was isolated. This protein was initially named ApxL2 but is now known as hShrm1.

Identification of hShrm1 full length cDNA. Two approaches were used. Firstly, based on the sequence of the 2H-clone7 (designated pACT2/2H-clone7), a specific primer (clone7-Race1: 5'-GAGGAGGTC-

ACTCTCTGCAGC TGTGG-3'; nt 1670 to 1645) was designed and used with Clontech SMART RACE (rapid amplification of cDNA ends) PCR system as recommended by the manufacturer. Secondly, a Blastn analysis performed with the 2H-clone7 sequence indicated this cDNA was encoded on chromosome 5 (P1 clone 1308e5, nt 2362–4259; GenBank accession no. AC004775). The genomic sequence overlapping this region was searched for potential exons and exon-intron boundary motifs using the FGENE and FGENESH programs (Genefinder package, Sanger Centre website). From this analysis, pairs of RT-PCR primers were designed: chr5–269 s (nt 269–291 in 1308e5, nt 1–23 in hShrm1) 5'-AGCGCTTGTGACGGTGTGACCAG-3' and chr-5–505as (nt 483–505 in 1308e5, nt 215–237 in hShrm1) 5'-ACAGGTCCAGGCTGCTAG TGGAC-3'; hShrm1/ATGs (nt 418–441 in 1308e5, nt 150–173 in hShrm1) 5'-TCAGCACTC ATCTGCGCAGC-CATG-3' and chr5–1375as (nt 1354–1374 in 1308e5, nt 1086–1107 in hShrm1) 5'-CCAAGACTTCGCCT-GAAGCGCT-3'; chr5–1354 s (nt 1354–1375 in 1308e5, nt 1086–1107 in hShrm1) 5'-AGCGCTT-CAGGCGAAGTCTTGG-3' and clone7-as (nt 2894–2913 in 1308e5, nt 2061–2080 in hShrm1). Hybridization temperatures were 58 °C for the first two primer sets and 56 °C for the last set. Amplified products were sub-cloned into pGEMTeasy (Promega, Madison, WI) and sequenced.

hShrm1 constructs. pACT2/2H-clone7 consists of the C-terminal domain of hShrm1 (nt 1614–3190) (GenBank accession no. AF314142) expressed as a GAL4-HA-fusion protein. The vector pCMV/hShrm1 was constructed by inserting the fragments NcoI-Eco47III (nt 170 to 1086), Eco47III-XhoI (nt 1087–1794) and XhoI-ApaL1 (nt 1795 to 2738) into pcDNA3.1(-) (Invitrogen, Carlsbad, CA). pHA/2H-hShrm1 consists of the original 2H-clone7 partial cDNA fused to a synthetic HA N-terminal tag and inserted between the EcoRI and HindIII sites of pcDNA3.1(-). RNA expression in pcDNA3.1-based constructs is under the control of either the CMV promoter for mammalian cell expression or the bacteriophage T7 promoter for *in vitro* translation assays. pHA/R744Stop was generated by performing site-directed mutagenesis on pHA/2H-Shrm1, changing arginine 744 (nt 2400) to a stop codon.

Northern blots. A human cancer cell line multiple tissue Northern (MTN) blot was from Clontech. RNA was hybridized with a 600 bp (nt 1614–2213) hShrm1 probe labeled randomly with [α-^{32}P] dATP using the prime-a-gene kit (Promega) and purified on Micro Bio-Spin 30 columns (Bio-Rad, Hercules, CA). Hybridization was for 60 min at 68 °C in HexpressHyb solution (Clontech). Filters were rinsed and washed 4x 10 min in 2x SSC, 0.05 % SDS at room temperature, then treated 2x 20 min in 0.1x SSC, 0.1 % SDS at 50 °C, exposed to a PhosphoImager screen and analyzed with the Storm 860 (Molecular Dynamics, Sunnyvale, CA). Filters were stripped and rehybridized with a β-actin probe.

Real-time PCR. Cells were grown to 80 % confluence in tissue culture, harvested and resuspended in RNAlater for storage (4 x 10^6 cells in 2 ml) (Ambion, Applied Biosciences, Foster City, CA). The cells were later centrifuged for 10 min at 3000 g, the supernatant discarded and the cell pellets resuspended in 350 µl RLT buffer. RNA was then extracted using the RNeasy Kit (QIAGEN, Hilden, Germany). Reverse Transcription (RT) was performed with 10µl RNA (1.5 µg) extracted from cells using Superscript II reverse transcriptase (Invitrogen). 4 µl of 5x First-Strand Buffer, 2 µl of 100 mM dithiothreitol, 1 µl of 50 µM random hexamers (Applied Biosystems), 1µl of dNTP 20 mM (GE Healthcare, Little Chalfont, UK), 1 µl sterile H_2O and 1 µl of Superscript II were added to 10 µl of RNA. The RT mix was incubated for 10 min at 24 °C, 1 h at 37 °C, 5 min at 95 °C and then frozen at -20 °C. For the quantitative real Time PCR (Applied Biosystems instrument: 7500 Fast Real-Time PCR System) a standard curve (5 dilutions) was done using cDNA extracted from HEK293 cells. The reaction mix contained 10 µl TaqMan® 2x Universal PCR Master Mix, 1 µl of probe, 2 µl cDNA and 7 µl H_2O. Each reaction was performed in triplicate. The PCR conditions were 2 min at 50 °C, 10 min at 95 °C, 15 s at 95 °C (40x) and 1 min at 60 °C. The probes were from Applied Biosystems. hCyclophylin: 4310885E: hShrm1: Hs00394595_g1;. The data were analyzed using the software provided with the instrument, and results normalized to cyclophylin.

Antibodies and *in vitro* translation. Rabbit anti-hShrm1 (α–hShrm1) was generated against the peptide SPS PAR PPG TCP PVQP (aa 825 – 840) by Eurogentec (Seraing, Belgium). Monoclonal (mAb) mouse anti-HA (α–HA, clone 12CA5) was from Roche Diagnostics and the anti-Penta·His (α–His) was from QIAGEN. [^{35}S]-labelled *in vitro* translated hShrm1 products were synthesized using the TnT-T7 quick coupled transcription/translation system (Promega) using either pHA/2H-hShrm1 or pHA/R744Stop circular DNA. To immunoprecipitate hShrm1, 16 µl of α–hShrm1 serum was added to the TnT mix and incubated overnight at 4 °C. Control experiments were performed with 16 µl of pre-immune (PI) serum, or α–HA or α–His mAbs at a final concentration of 2 ng/µl. The immunocomplexes

were collected with protein A-Agarose (rabbit antibodies) or protein G-Agarose (mouse mAbs)(Roche Diagnostics), washed extensively with IP buffer, and then eluted in sample buffer. Proteins were separated on SDS-PAGE and the gels analyzed by autoradiography or the Storm 860.

Binding and co-immunoprecipitation studies, Western blotting. The MCAM cytoplasmic tail and the β-adrenergic receptor C-tail fragment were subcloned into pcDNA3.1 (His) (Invitrogen) to generate the 6xHis-tagged expression vectors pHis/MCAM and pHis/β-adren-Ct, respectively. They were co-transfected into COS-7 cells with pHA/2H-hShrm1. Cell extracts were prepared in lysis buffer and incubated with Ni-agarose beads for 2 h at 4 °C. Beads were washed (4x) in high salt buffer (50 mM NaH_2PO_4, 300 mM NaCl, 10 mM imidazole). Bound proteins were eluted with SDS-sample buffer containing 250 mM imidazole, separated on SDS-PAGE and blotted with α-His (1:2000) or α-HA (1:2000) mAbs, followed by anti-mouse Ig HRP-conjugated antibody and ECL detection (GE Healthcare).

For co-immunoprecipitations, hShrm1 was over-expressed by transfecting SK-Mel28 melanoma cells with a full-length hShrm1 plasmid construct. Cell lysates were prepared in Brij 97 buffer (50 mM Tris-HCl pH 7.6, 100 mM NaCl, 1 % Brij 97 and Complete Protease Inhibitor (Roche Diagnostics)). Lysate (200 µl) was pre-cleared by mixing with Protein G sepharose beads (GE Healthcare) and then mixed for 2 h at 4 °C with either 4 µl of α−hShrm1 immunoglobulin (800 µg/ml, purified from anti-serum by a protein A affinity procedure), PI-serum (1/30 dilution), 6 µl of the α−MCAM mAb CC9.c19 (CC9) (500 µg/ml) (a gift from Andrew Zannettino, Hanson Center for Cancer Research, Adelaide, South Australia) [26] or 6 µl α-mouse IgG_{2a} control (500 µg/ml; Zymed). Protein G beads captured the immunocomplexes. Beads were washed in Tris-buffered 100 mM NaCl containing 0.5–1.0 % Brij 97 followed by buffer without Brij 97. Eluted proteins were separated on 7.5 % SDS-PAGE, electro-blotted and the blots probed with biotinylated CC9 mAb (2 µg/ml) and streptavidin-HRP (GE Healthcare). Proteins were visualized using ECL detection.

Triton-X-100-insoluble and soluble cell fractions were separated by centrifugation (100 000 g for 1 h at 4 °C) of melanoma cell lysates prepared in a Triton-X-100 buffer (20 mM Tris-HCl, 150 mM NaCl, 5 mM EDTA, 200 mM sucrose and 1 % Triton-X-100). Fractions were solubilised in SDS sample buffer, separated on SDS-PAGE, electro-blotted and the blots probed with the α−MCAM mAb CC9 (2.5 µg/ml) and α−hShrm1 antibody (4 µg/ml) or, as a control, with a mouse α−human vinculin mAb, (clone V284; Chemicon, Millipore, San Francisco, CA). Triton-X-100 extracts were prepared from cells plated for 1.5 h on dishes coated with fibronectin (10 µg/ml, Sigma-Aldrich) or polyhema (Sigma-Aldrich) according to the manufacturers' instructions.

Immunofluorescence. Cells were grown on coverslips coated with 10 µg/ml fibronectin (Sigma-Aldrich) and fixed with 2 % paraformaldehyde in PBS. Cells were permeablised with 0.1 % Triton-X 100 for 3 min at 4 °C. Primary antibodies were α-hShrm1 serum (1:30); α-CD146 (5 µg/ml) (clone P1H12; Chemicon, Millipore); mAb CC9 (α-MCAM; 5ug/ml) and α-β-actin (5 ug/ml) (clone AC-15, Sigma-Aldrich); and as controls: PI-serum (1:30) or mouse IgG_1 (5 µg/ml) (Zymed Laboratories, Invitrogen). Cells were blocked with 1 % BSA/PBS and then incubated with the primary antibodies, prepared in 1 % BSA/PBS, for 1 h at room temperature. Coverslips were washed, then reacted with either fluorescein (FITC)-conjugated goat α−rabbit IgG F(AB')2 (Cappel, MP Biomedicals, Solon, OH) or Alexa Fluor 488 or 546 α−mouse IgG_1or IgG2a (Molecular Probes, Invitrogen) for 1 h at room temperature. Coverslips were mounted in Vectashield (Vector Laboratories, Burlingame, CA) and the images captured using a MRC 1024 UV Laser Scanning Confocal Microscope (Bio-Rad).

Bioluminescence resonance energy transfer (BRET). The following fusion constructs were made. hShrm1-Rluc (N-tagged) was made by amplifying, from cDNA obtained from SK-Mel28 cells, full length hShrm1 using primers containing appropriate restriction sites. This fragment was ligated, in frame, into pcDNA3.1 3' to the coding sequence of the *Renilla* luciferase (Rluc) gene, creating a fusion construct with Rluc at the N-terminus of hShrm1. hShrm1-Rluc constructs lacking the proline rich region and/or ASD2 were prepared as above, using reverse primers that generated a truncated protein and included a stop codon. MCAM-EGFP (C-tagged) was made by amplifying, from cDNA obtained from SK-Mel28 cells, full length MCAM using primers with appropriate restriction sites. The reverse primer removed the stop codon. This fragment was ligated in frame into pcDNA3.1, 5' to the coding sequence of enhanced green fluorescent protein (EGFP) to create a fusion construct with EGFP at the C-terminus of MCAM. MCAM constructs with cytoplasmic tail deletions were generated as above, using reverse primers within the MCAM cytoplasmic tail to produce truncated MCAM-EGFP fusion proteins. MCAM constructs containing mutations in the endocytosis motifs were generated by site directed mutagenesis using *Pfu* Turbo polymerase (QuikChange protocol, Stratagene, USA). The first

leucine of the di-leucine domain was changed to a proline (MCAM-LP-EYFP) and the tyrosine in the tyrosine based motif to glycine (MCAM-Tyr-EYFP). The control plasmids were pcDNA3.1/Rluc, pcDNA3.1/EGFP and thyrotropin releasing hormone receptor (TRHR) EGFP, which have been described [27]. HEK293 cells were grown in six-well plates and when 90% confluent were transfected with control (empty Rluc vector or empty EGFP vector), MCAM and hShrm1 constructs using Lipofectamine^{2000} (Invitrogen) and left for 24–48 h. For BRET analysis 10^5 cells in 100 µl were placed into the wells of a white 96-well plate. Coelenterazine (Molecular Probes, Invitrogen) was added at 5µM; and luminescence was measured at 440–500nm and 510–590nm over a 1–5 min time-course. A BRET ratio was calculated and normalized to the BRET ratio obtained from the Rluc only control sample [27]. This ratio indicates the proximity of the two tagged constructs [28].

For every BRET experiment, the expression of the EGFP-tagged constructs was measured using flow cytometry. The expression of fusion constructs expressed in HEK293 cells was also examined using SDS-PAGE and Western blotting. The α-EGFP antibody (clone JL-8) was purchased from Clontech and α-RLuc (clone 1D5.2) from Chemicon (Millipore).

Results

Expression of the Long and Short Cytoplasmic Variants of MCAM. Two MCAM splice variants, MCAM-L and MCAM-S, were found to be expressed in endothelial cells [13] (Fig. 1). Bioinformatic analysis of the MCAM cytoplasmic tail revealed two protein kinase C (PKC) phosphorylation sites at R592 (RGSK) and K612 (KSDK) and two endocytosis signals. A tyrosine-based endocytosis motif was identified at Y640 that conforms to the consensus YXX∅ (where Y is a tyrosine, X is any amino acid and ∅ is an amino acid with a bulky hydrophobic group) and a di-leucine motif at position L622 [29, 30] was identified. MCAM-S is formed by deletion of exon 15 and results in the loss of both endocytosis motifs and one of the PKC sites. The fusion between exons 14 and 16 also creates a PDZ domain interaction site.

Using hMCAM-specific oligonucleotides, we observed by RT-PCR that, although both of these transcripts are present in a variety of cell lines (Fig. 2A), MCAM-L was more easily detected than MCAM-S in melanoma cells (Fig. 2B).

Isolation of hShrm1 by the yeast two-hybrid system. To identify factors that interact with the cytoplasmic tail of MCAM in melanoma cells, we performed a yeast two-hybrid screen of a human brain library (in which MCAM is highly expressed) using the cytoplasmic tail of MCAM-L as bait (Fig. 1B). One partial cDNA clone (2H-clone7) was isolated. Co-transformation in yeast of the MCAM bait together with 2H-clone7 produced a moderate but consistent increase in β-galactosidase activity compared to that detected when 2H-clone7 was transformed alone or with the control bait, or when the MCAM and control baits were expressed alone (Fig. 3). These data indicate an interaction between the cytoplasmic tail of MCAM and 2H-clone7.

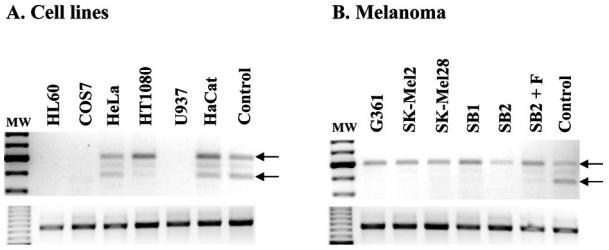

Figure 2. Expression of the MCAM cytoplasmic variants in human cells. Total RNA from non-melanoma (*A*) and melanoma (*B*) cell lines was analysed by RT-PCR. After 32 cycles of amplification the products were separated by electrophoresis on 2% agarose and visualised using ethidium bromide. The long form appears as the upper band (600 bp) and the short form as the lower band (482 bp) (indicated by the arrows). The control in A and B is total RNA from normal brain. MW is a 100 bp molecular weight marker. Amplification of β-actin (838 bp) (lower panel) was used as a control for mRNA integrity.

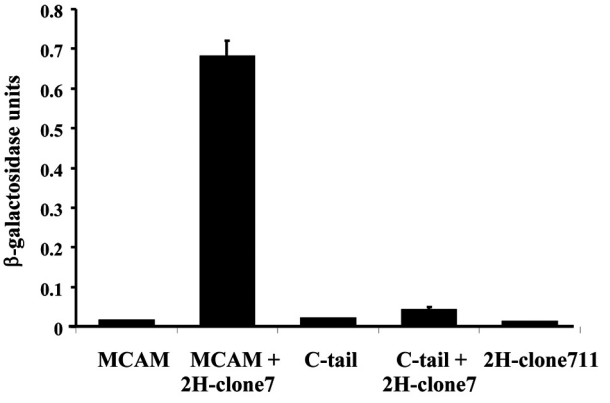

Figure 3. MCAM bait together with 2H-Clone 7 shows expression of β-galactosidase activity. Yeast Y153 cells were transformed with pAS1/MCAM as bait, alone or together with the pACT2-based 2H-clone7 vector. Similar transformations were performed with a control fragment corresponding to the cytoplasmic domain of the β-adrenergic receptor inserted in pAS1 (C-tail), with or without 2H-clone7 DNA. pACT2/2H-clone7 was also transformed alone. Transformants were assayed by a liquid β-galactosidase assay as described in Materials and methods. Data are mean ± standard error of three experiments in duplicate.

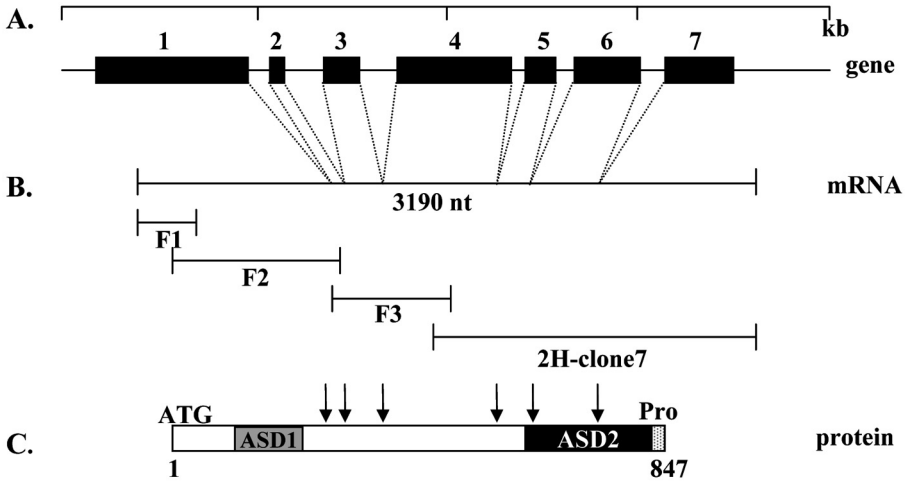

Figure 4. Structure of hShrm1. (*A*) Genomic organization of the hShrm1 gene. The ≈ 4 kb gene is based on the alignment of the sequence of the putative hShrm1 transcript with the sequence of the chromosome 5 P1 clone 1308e5 (GenBank accession number no. AC004775). Filled boxes numbered 1–7 indicate exons. (*B*) hShrm1 mRNA. The structure of the putative 3190 nt hShrm1 transcript results from assembling the sequences of the original brain 2H-clone7 cDNA fragment identified in the two-hybrid screen with the fragments F1, F2 and F3 amplified by RT-PCR from brain total RNA. (*C*) hShrm1 protein. The 847 amino acids ORF encoded by the 3190 nt mRNA is shown. ASD1 and ASD2 are indicated by the grey box and black box respectively. Pro-: proline-rich region and vertical arrows indicate exon junctions.

The 2H-clone7 cDNA shows sequence homology with the chromosome 5 clone P1 1308e5 (GenBank accession no. AC004775). Based on the sequence of 2H-clone7, a 5'-RACE primer was designed, which amplified extra 5' sequences from total brain RNA matching chromosome 5, P1 1308e5 clone. However, using the RACE approach, we were not successful in identifying full-length mRNA transcripts. The region of the chromosome 5 clone P1 1308e5 encoding the 2H-clone7 cDNA fragment was then searched for potential exons and exon-intron boundaries. Based on this analysis, three pairs of RT-PCR primers were designed to amplify total brain RNA. Assembling the resulting fragments with 2H-clone7 created a 3190 bp cDNA transcript encoding an open reading frame (ORF) of 847 amino acids (nt 171 to 2714) with a calculated Mr of 90.3 (Fig. 4). The sequence overlapping the start methionine conforms to the consensus for translation initiation site [31]. A stop codon located upstream of this methionine at nt 36 indicates that the 847 amino acids ORF probably represents a full length product.

BLAT analysis [32] of the 3190 bp sequence indicated that the product we isolated was identical to hShrm1 as defined by the Genome Browser at UCSC [33] and the NCBI databases [34].

hShrm1 expression. Northern blot analysis using as a probe a 600 bp fragment corresponding to most of the original 2H-clone7 cDNA revealed three mRNA species. A main 3.3 kb transcript and two larger species of 6.5 and 8.5 kb were detected in polyA(+) RNA from various cell lines including G361 melanoma, HeLa cervix carcinoma and K-562 chronic myelogenous leukemia cells (Fig. 5A). In contrast, hShrm1 transcripts were absent from promyelocytic leukemia HL60, from lymphoblastic leukemia MOLT4 or from Burkitt's lymphoma Raji cells. hShrm1 mRNAs were also detected in brain, heart, skeletal muscle, colon, small intestine, kidney, placenta and lung tissues, but in lower amounts than those observed in cell lines (data not shown). Thymus, spleen and peripheral blood mononuclear cells were hShrm1 negative. To confirm the Northern blot analysis, we performed RT-PCR using specific hShrm1 oligonucleotides (Fig. 5B). After 35 cycles of amplification, hShrm1 transcripts were detected at low levels in healthy human tissues, whereas hShrm1 transcripts were clearly present in the melanoma G361 cell line and in a range of tumour tissues (Fig. 5B).

To investigate whether hShrm1 expression levels as measured by mRNA were correlated with cell surface MCAM protein expression, quantitative real time PCR was performed. The ratio of hShrm1: hCyclophylin expression was compared between four melanoma cell lines expressing different levels of cell surface MCAM. By flow cytometry using the CC9 mAb the order of MCAM expression on the surface of these melanoma cells from lowest to highest was MM253, A2058, SK-Mel28 and MM96L. Primary human keratinocytes were MCAM negative and HUVECs were strongly MCAM positive (unpublished data). The ratio of hShrm1: hCyclophylin mRNA was found to be between 0.28 and 0.52 for the melanoma cell lines and the

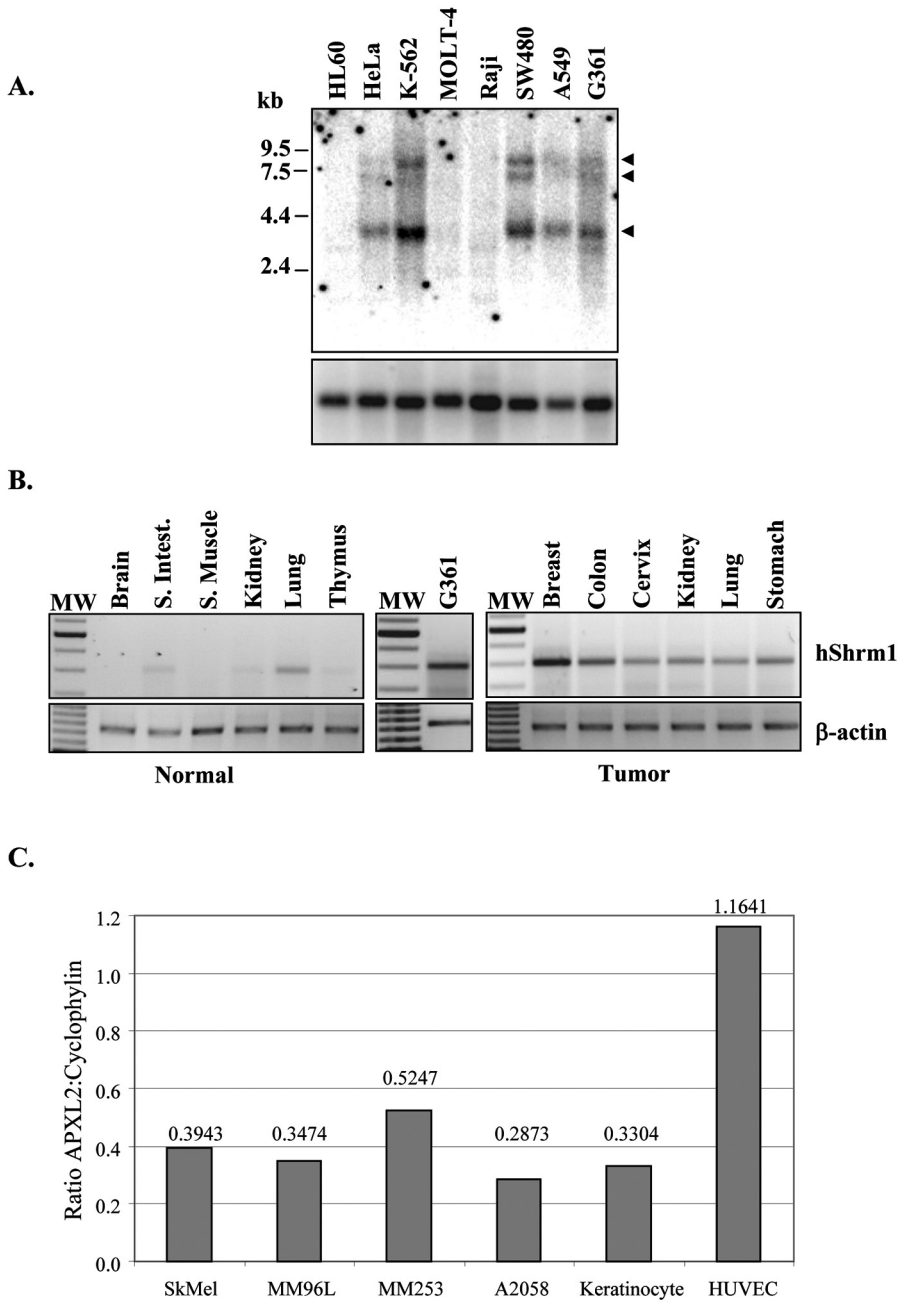

Figure 5. hShrm1 mRNA expression. (*A*) Northern blot analysis. Poly(A)$^+$ RNA from the indicated cell lines was hybridized with 2H-clone7 cDNA as probe. The three transcripts (8.5, 6.5 and 3.3 kb) are indicated with arrowheads. Lower panel: filters were stripped and rehybridized with β-actin. (*B*) RT-PCR analysis. Human normal or tumor total RNA (100 ng) from the indicated tissues or from the melanoma cell line G361 were analyzed by RT-PCR using the clone7-s and clone7 s-as oligonucleotides as primers. After 35 cycles of amplification, products were analyzed by electrophoresis on 2% agarose and stained with ethidium bromide. β-actin was used as control for mRNA integrity. MW: 100 bp ladder. (*C*) Quantitative real-time PCR. RNA was extracted from a variety of human melanoma cell lines, primary keratinocytes and HUVECs. A TaqMan assay was performed using probes against hShrm1 and hCyclophylin. hShrm1 expression was normalised to hCyclophylin expression in each cell line.

keratinocytes, and was not correlated with MCAM cell surface expression levels (Fig. 5C). Interestingly, HUVECs showed the highest ratio of hShrm1:hCychophylin expression of 1.16.

The hShrm1/MCAM Interaction. To characterize hShrm1 biochemically, a rabbit antiserum was generated against a 16 amino acid motif in the C-terminal proline-rich region of hShrm1. Anti-hShrm1 (α−hShrm1) serum and α−HA antibodies, but not pre-immune (PI) serum or α−His antibodies, immunoprecipitated *in vitro* translated HA-tagged hShrm1 (Fig. 6A). In contrast, synthetic HA/hShrm1 fusion proteins lacking the C-terminal proline-rich region were not recognized by α−hShrm1 serum but they were immunoprecipitated with α−HA (Fig. 6A). To analyze whether the C-terminal region of hShrm1 interacted with the MCAM cytoplasmic tail, an *in vivo* binding assay was performed. An HA-tagged/hShrm1 fusion expression vector (pHA/2H-hShrm1), based on the original 2H-clone7 cDNA, was transfected in COS-7 cells either alone, with the 6xHis-tagged/MCAM fusion expression construct pHis/MCAM or, as a control, the 6xHis-tagged C-terminus of the β-

adrenergic receptor (pHis/β-adren-Ct). Cell lysates were prepared and incubated with Ni^{2+}-agarose beads to precipitate the histidine tag containing proteins. Figure 6B shows that hShrm1 was co-purified with MCAM, but not with the control protein, confirming the interaction between hShrm1 and MCAM.

Co-immunoprecipitation studies using the melanoma cell line SK-Mel28 were performed to investigate whether native MCAM and hShrm1 associated *in vivo*. Analyses Western blot indicated that the α-MCAM mAb CC9, stained a band of molecular weight around 120 kDa, whereas the α-hShrm1 antibody stained a band of approximately 80 kDa (Fig. 6C). These two bands are the expected sizes of MCAM and hShrm1, respectively. Immunoprecipitating with the α-MCAM mAb CC9 and blotting with biotin-labelled CC9 produced a strong band at 120 kDa (Fig. 6D). When α-hShrm1 was used as the immunoprecipitating antibody a band of 120kDa was also detected using biotin-labelled CC9, indicating that hShrm1 and MCAM co-immunoprecipitate (Fig. 6D). However, the difference in intensity of these two bands suggests that most of the MCAM in SK-Mel28 cells is not complexed with hShrm1.

Confocal immunofluorescence microscopy was used to analyse the cellular distribution of hShrm1 and MCAM. SK-Mel28 and A2058 melanoma cells were stained with α−hShrm1 anti-serum and the α-MCAM mAb CC9 (Fig. 7). These experiments revealed clear cytoplasmic staining with the α−hShrm1 anti-serum concentrated in the perinuclear region, whereas staining from the α-MCAM mAb CC9 was extensively distributed throughout the cytoplasm and on the cell membrane. The merged images confirm that a proportion of hShrm1 does co-localize with MCAM and this occurs primarily in the perinuclear region.

The *in vivo* interaction of MCAM and hShrm1 was also investigated using bioluminescence resonance energy transfer (BRET) [27, 28]. BRET occurs between the donor molecule Rluc and acceptor molecule EGFP in the presence of coelenterazine, a cell permeable substrate oxidised by the enzyme Rluc to yield blue light at 480 nm. Energy transfer occurs when Rluc is in close proximity to EGFP (<100 Å) and leads to the emission of yellow/green light (510−590 nm). A BRET signal is measured by the amount of yellow/green light emitted by EGFP compared with the blue light emitted by Rluc upon addition of coelenterazine to cells transfected with Rluc and EGFP fusion constructs. The BRET ratio increases as the ratio of yellow/green light: blue light increases as the two proteins interact. An increase in BRET ratio of test sample over an Rluc alone control sample indicates that the two tags are in very close proximity and hence, the proteins carrying these tags are interacting.

To confirm the integrity of the proteins produced by the fusion constructs used in the BRET experiments, HEK293 cells were transfected separately with the EGFP and Rluc constructs. Cell lysates were made and analysed via SDS-PAGE and Western blotting, using α−GFP and α−Rluc antibodies. All constructs produced proteins of approximately the correct size, with the hShrm1 fusion proteins showing a tendency to dimerise, as does the native protein (data not shown). All EGFP constructs were examined using fluorescent microscopy to confirm that MCAM-EGFP and hShrm1-EGFP showed expression patterns similar to native proteins. In particular, it was confirmed that all of the MCAM constructs showed cell surface expression similar to wild type MCAM (data not shown).

HEK293 cells co-transfected with hShrm1-Rluc (N-tag) and MCAM-EGFP (C-tag) expression constructs showed moderate but consistent increases in BRET ratio compared to HEK293 cells transfected with hShrm1-Rluc (N-tag) alone; or co-transfected with hShrm1-Rluc (N-tag) and TRHR-EGFP (C-tag) fusion protein, an unrelated membrane bound protein (Fig. 8A). These data further support the conclusion that hShrm1 and MCAM interact in a mammalian cell system.

To investigate which regions of the cytoplasmic tail of MCAM play a role in the interaction between hShrm1 and MCAM, a number of MCAM mutants and deletion constructs were generated to test in the BRET system. When transfected into HEK293 cells, the mutant proteins appeared to interact with hShrm1 to the same extent as wild type MCAM, as similar BRET ratios were obtained in cells transfected with hShrm1-Rluc (N-tag) and either the wild type MCAM-EGFP (C-tag), MCAM-Tyr-EYFP (C-tag) or MCAM-LP-EGFP (C-tag) constructs (Fig. 8A). In all three cases the BRET ratio was consistently markedly higher than that obtained with HEK293 cells transfected with hShrm1-Rluc (N-tag) alone; or with hShrm1-Rluc (N-tag) and TRHR-EGFP (C-tag). MCAM tail deletion constructs that lacked either the tyrosine sorting motif or both the tyrosine and di-leucine sorting motifs also appeared to interact with hShrm1 to the same extent as wild type MCAM, as these constructs all produced BRET ratios similar to wild type MCAM and significantly higher than control TRHR-EGFP (C-tag) (Fig. 8A). However, a deletion construct that lacked the entire cytoplasmic tail, except for a cluster of basic amino acids immediately adjacent to the trans-membrane domain (KKGK, Fig. 1), failed to interact with hShrm1. HEK293 cells transfected with hShrm1-Rluc (N-tag) and MCAM-

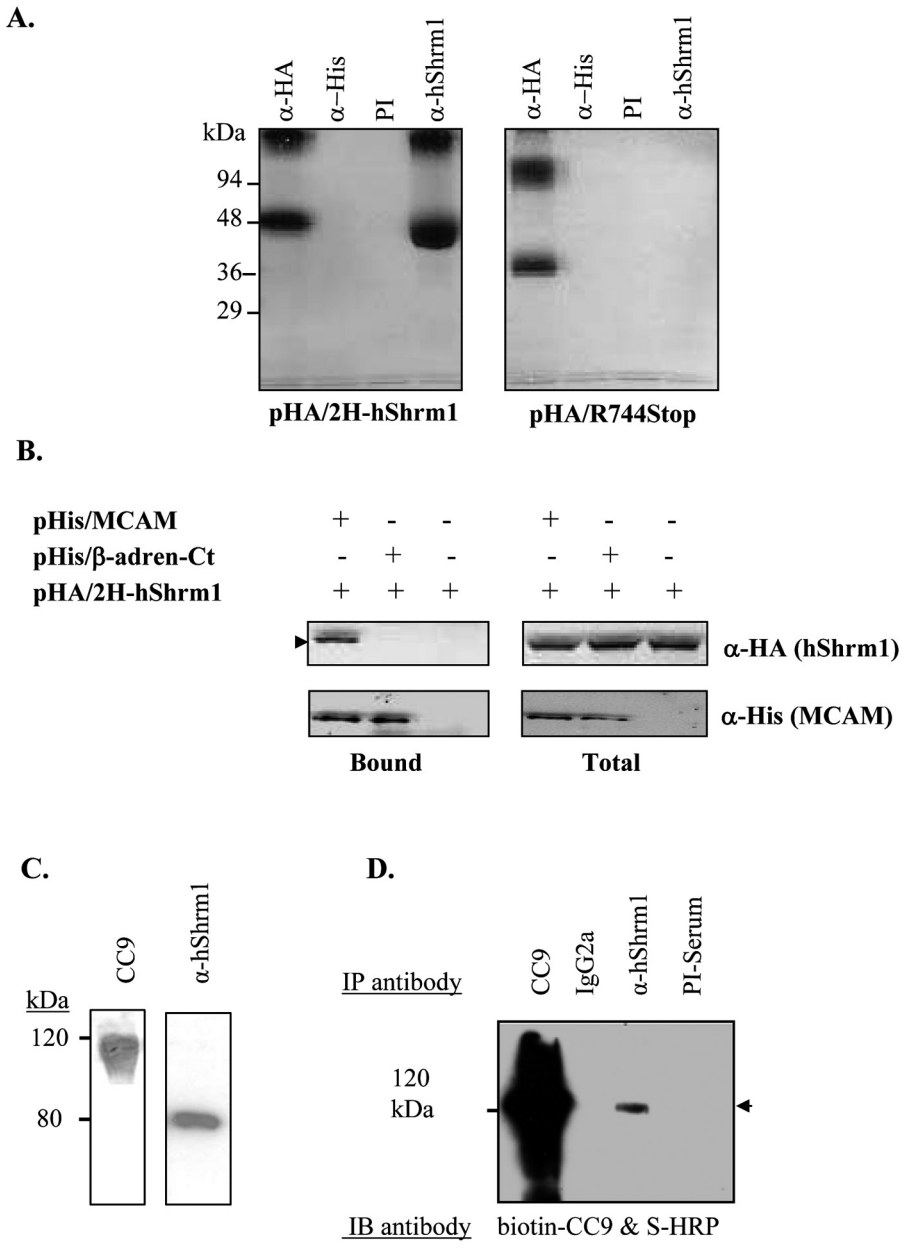

Figure 6. Immunoprecipitation of hShrm1 and co-immunoprecitation of hShrm1 and MCAM. (*A*) The plasmids pHA/2H-hShrm1 (encoding the original 2H-clone7 cDNA tagged with the HA epitope) or pHA/R744Stop (with a stop codon interrupting the reading frame upstream of the proline-rich region) were used as templates to prepare *in vitro* TnT ^{35}[S]-labeled proteins. The TnT products were incubated either with a rabbit antiserum directed against the peptide motif SPS PAR PPG TCP PVQP located within the proline-rich region (α–hShrm1), or as controls either with anti-Ha (α–HA), anti-His (α–His) or pre-immune (PI) serum, and the immunocomplexes were collected with protein A agarose (α–hShrm1 and PI) or protein G agarose (α–HA and α–His). Precipitated proteins were separated on 10% SDS-PAGE. The lower bands are the immunoprecipitated product. The top bands probably represent read-through products in the TnT system. (*B*) Co-immunoprecipitation of 2H-hShrm1 with the MCAM cytoplasmic tail. 2H-hShrm1 was expressed in COS-7 cells as a HA-tagged fusion protein either alone or together with the MCAM cytoplasmic tail or a control cytoplasmic-tail fused to the His epitope. Cell lysates were analysed by immunoblotting either directly (total) or after purification on Ni-agarose beads (bound). Blots were probed either with α–HA (upper panels) or α–His (lower panels) antibodies. The arrowhead indicates hShrm1, which was co-purified with MCAM on the Ni-agarose beads. (*C*) Co-expression of hShrm1 and MCAM in melanoma cells. Total cell lysates of SK-Mel28 cells were analysed by Western blotting, with the membranes probed with α–MCAM biotin-labeled mAb, CC9, or with purified α-hShrm1. (*D*) Co-immunoprecipitation of full length MCAM and hShrm1 in SK-Mel28 melanoma cells. Proteins were immunoprecipitated from total cell lysate using either the α–hShrm1 antibody, or the α–MCAM mAb CC9. Mouse IgG2a antibody and pre-immune (PI) serum were used as controls. Immunoprecipitated proteins were analyzed by immunoblotting with biotinylated CC9. The 120 kDa band corresponding to immunoprecipitated MCAM is shown with an arrow head; MCAM has co-precipitated with hShrm1. IP antibody: antibody used for immunoprecipiatation. IB antibody: antibody used for immunoblotting.

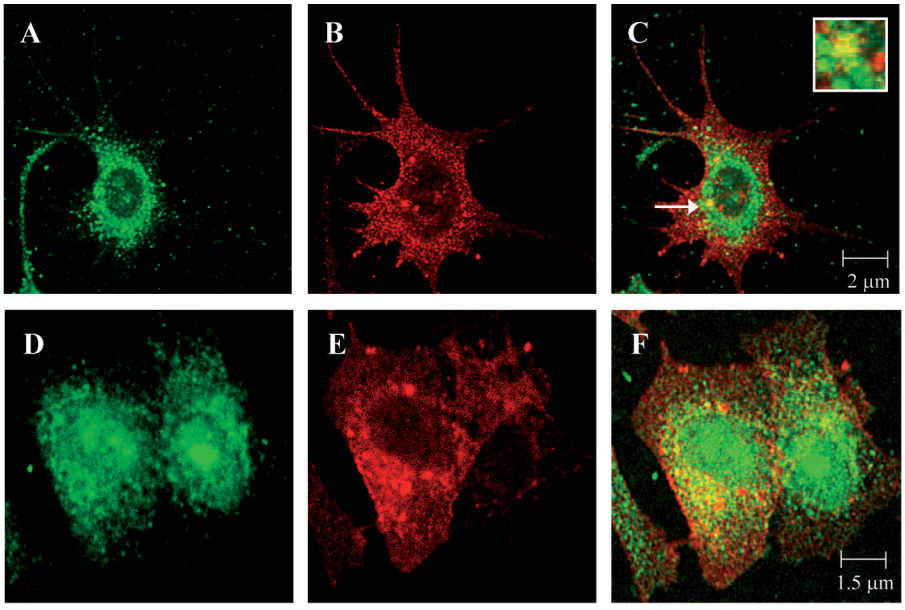

Figure 7. Localisation of MCAM and hShrm1 in melanoma cells. Cells were stained with α-hShrm1 and FITC-conjugated goat α-rabbit IgG F(AB') (*A* and *D*) and α-MCAM, clone P1H12 and Alexa-Fluor 546 α-mouse IgG1 (*B* and *E*) antibodies. SK-Mel28 (*A – C*) and A2058 (*D – F*) cells were visualized using confocal microscopy, with images taken of an identical field of view in different colour channels showing the localization of hShrm1 and MCAM. These images were superimposed to generate the composite images (*C* and *F*). Arrows (*C*) indicate an area of co-localisation, which are also shown enlarged and boxed.

tail-less-EGFP (C-tag) showed BRET ratios equal to those obtained with HEK293 cells transfected with hShrm1-Rluc (N-tag) and control TRHR-EGFP (C-tag). This indicates that hShrm1:MCAM binding may be mediated by the 30 amino acids that lie between the basic amino acids adjacent to the transmembrane domain and the di-leucine motif.

To determine which regions of hShrm1 were involved in the hShrm1:MCAM interaction we generated two deletion constructs of hShrm1. hShrm1-del-Pro-Rluc (N-tag) lacked the C-terminal poly-proline region and hShrm1-del-ASD2-RLuc (N-tag) lacked both the poly-proline and ASD2 motifs. Co-transfection of either of these hShrm1-Rluc (N-tag) deletion constructs with MCAM-EGFP (C-tag) in HEK293 cells produced a similar BRET ratio to that obtained in cells transfected with wild type hShrm1-Rluc (N-tag) and MCAM-EGFP (C-tag) (Fig. 8B). This suggests that neither the proline rich region nor ASD2 are necessary for the hShrm:MCAM interaction in mammalian cells.

Association of hShrm1 with the cCytoskeleton. To investigate whether hShrm1 associated with the actin cytoskeleton in melanoma cells the selective extraction of hShrm1 and MCAM with Triton X-100 was examined. Insolubility in Triton X-100 is a common indicator of cytoskeletal association [35]. Triton X-100 soluble and insoluble fractions were prepared from A2058 and SK-Mel28 melanoma cells that were either allowed to spread on fibronectin or were made to remain spherical by plating on polyhema. These fractions were examined for hShrm1 and MCAM content by Western blotting (Fig. 9A). The distribution of these two proteins was similar in both melanoma cell lines. Most of the MCAM was found in the soluble fraction but a clear band was also consistently detected in the insoluble fraction when the cells were spread on fibronectin. In contrast, hShrm1 was found exclusively in the insoluble fraction obtained from these cells, suggesting that it associates with the cytoskeleton regardless of whether the cells were spread (on fibronectin) or spherical (on polyhema). Similar to MCAM, vinculin was located in the soluble fraction when the cells were spherical, but was also found in the insoluble cytoskeletal fraction when cells were spread on fibronectin. The distribution patterns of these proteins indicate that hShrm1 very likely associates with the cytoskeleton as these data cannot be explained by incompletely solubilised and pelleted membrane fragments or by the non-specific trapping of hShrm1.

An examination of the possible interaction of hShrm1 with the cytoskeleton by confocal microscopy supported the conclusions derived from Figure 9A. In A2058 melanoma cells, merged images of cells stained with α-hShrm1 and α-β-actin mAb indicate some co-localisation of hShrm1 and β-actin (Fig. 9B).

Discussion

We have shown that the two MCAM splice variants described in endothelial cells (Fig. 1) [13] are expressed in a wide range of cell lines and that MCAM-L is the predominant variant in melanoma cells (Fig. 2). MCAM has been well characterised as a cell surface adhesion molecule and is positively correlated with metastatic potential in melanoma cells [14, 15, 36].

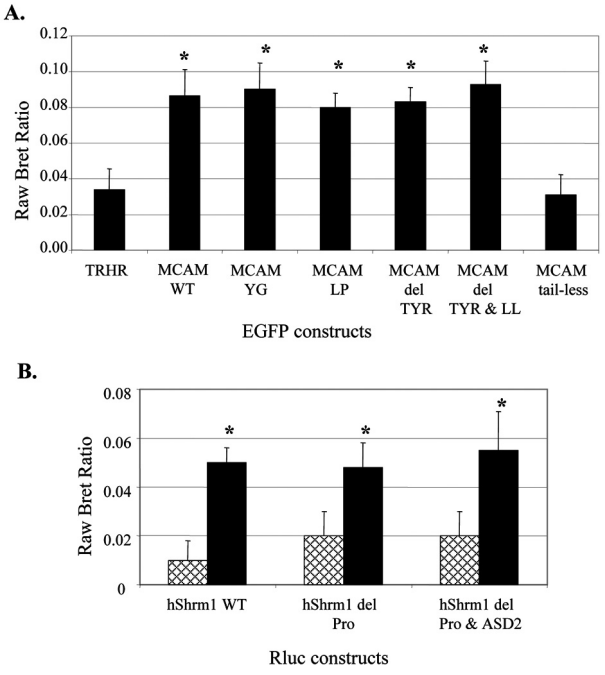

Figure 8. Interaction of ApxL2 and MCAM in vivo. (*A*) BRET was measured in HEK293 cells transfected with ApxL2-Rluc (N-tag) alone (control samples) or HEK293 cells co-transfected with ApxL2-Rluc (N-tag) and a range of EGFP (C-tag) constructs. The MCAM-EGFP (C-tag) constructs were MCAM WT (wild type), MCAM YG (tyrosine motif mutant), MCAM LP (di-leucine motif mutant), MCAM del TYR (no tyrosine motif), MCAM del TYR & LL (neither sorting motif) and MCAM del tail (lacking the entire cytoplasmic domain). Thyrotropin releasing hormone receptor (TRHR)-EGFP (C-tag) was a control construct. (*B*) BRET was measured in HEK293 cells transfected with either hShrm1-Rluc (N-tag), hShrm1 del Pro (N-tag) (lacking the proline rich region) or hShrm1 del Pro & ASD2 (N-tag) (lacking both the proline rich and ASD2 regions) alone or in combination with TRHR-EGFP (C-tag) or MCAM WT EGFP (C-tag). HEK293 cells co-transfected with hShrm1-Rluc (N-tag) constructs and MCAM WT EGFP (C-tag) (black bars) are compared to HEK293 cells co-transfected with hShrm-Rluc (N-tag) constructs and TRHR EGFP (C-tag) (hatched bars). (A and B) HEK293 cells were incubated with 5 μm coelenterazine and BRET readings were obtained every minute for 5 min. Data shown are BRET ratios normalized to the BRET ratio obtained with cells transfected with MCAM-Rluc WT (C-tag) alone. Data are representative of three separate experiments. Means + SD are shown. * denotes a statistically significance difference ($p<0.05$, Student's t-test) between the mean BRET ratios of each construct compared to the control BRET ratio.

However, little was known about its intracellular binding partners or possible signalling pathways, which was the rationale for using the cytoplasmic tail of MCAM-L as bait in a yeast-two-hybrid screen of a human brain cDNA library. This screen identified hShrm1 as a putative intracellular binding partner of MCAM-L (Fig. 3).

The putative interaction between hShrm1 and MCAM was then investigated in mammalian cells using co-immunoprecipitation, BRET and immunofluorescence microscopy. These experiments confirmed that hShrm1 and MCAM do interact *in vivo* (Figs. 6D, 7 and 8). Furthermore, we have demonstrated that hShrm1 is found in the Triton X-100 insoluble fraction of melanoma cell extracts and partly co-localises with β-actin (Fig. 9). These data suggest that hShrm1, like other members of the Shrm protein family, interacts with the actin cytoskeleton. Thus, we propose that hShrm1 is involved in linking MCAM to the cytoskeleton.

hShrm1 is an 80–90 kDa protein that belongs to the Shrm family of actin binding proteins. This protein family is based on the conservation of a specific arrangement of an N-terminal PDZ domain, a central ASD1 motif and a C-terminal ASD2 motif (Fig. 10A). The ASD1 and ASD2 domains are unique to the Shrm1 family. In several family members the ASD1 motif appears to be important for binding actin, the ASD2 motif for apicobasal constriction and PDZ in subcellular targeting [2]. Although the first member of the Shrm family, xShrm1 (Apx) was described in 1992 [4], the relationship between the members of this family has only recently become more apparent. The data to date suggest that the Shrm family can be divided into at least four sub-families (Shrm1–4) (Fig. 10B) based on structural similarities [1]. Proteins belonging to the Shrm2 and Shrm3 sub-families contain all three domains (PDZ, ASD1 and ASD2) and although the PDZ motif is important in directing subcellular targeting of Shrm2 it appears to be non-essential in Shrm3 [7, 9, 37]. In contrast, Shrm4 proteins lack a discernable ASD1 motif and hShrm1 and xShrm1 lack the PDZ domain (Fig. 10A). The ASD2 domain is the common feature of all currently described Shrm family proteins [1, 2].

Hagens et al. (2006) proposed that hShrm1 is the likely homologue of xShrm1 (*Xenopus*), as both of these proteins lack the PDZ domain present in Shrm proteins 2, 3 and 4 [1]. However, Yoder and Hildebrand (2007) disagree and state that xShrm1 differs from other Shrm family members and may not have homologues in other species [2]. To further investigate the relationship between xShrm1 and the hShrm proteins we performed multiple sequence alignment of the ASD2 domains, as this is considered the most conserved region in Shrm proteins (Clustal W) [38]. This basic analysis indicated that the ASD2 domain of xShrm1 shows greater similarity to the ASD2 domains of hShrm 2, 3 and 4 than it does to the ASD2 domain of hShrm1 (51%, 54% and 46% versus 35%, respectively). In addition, the ASD2 domain of hShrm1 shows relatively low similarity to the ASD2 domains of hShrm 2, 3 and 4 (38%, 33% and 32%).

In light of this analysis, we suggest that hShrm1 is not the human homologue of xShm1 and may instead belong to a novel sub-family of Shrm proteins.

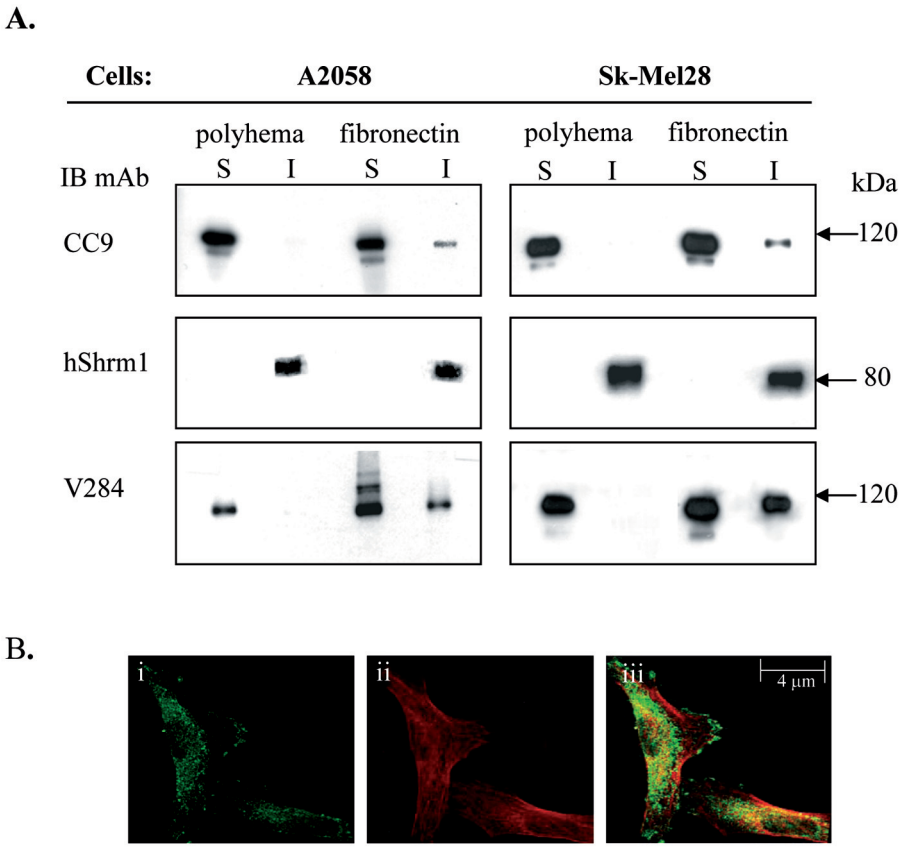

Figure 9. Association of hShrm1 and MCAM with the cytoskeleton of melanoma cells. (*A*) A2058 and SK-Mel28 melanoma cells plated on either polyhema or fibronectin were lysed in 1% Triton X-100, and the triton-insoluble fraction and the soluble supernatant were isolated by centrifugation as described in the Materials and methods. Proteins from the indicated subcellular fractions were electrophoresed, immunoblotted with the α-MCAM mAb, CC9 (top panel), α−hShrm1 (middle panel) or the α-vinculin mAb, V284 (bottom panel). Triton-soluble supernatant (S) and insoluble cytoskeletal pellet (I). (*B*) Localisation of hShrm1 and β-actin in A2058 melanoma cells; Cells were stained with α−hShrm1 and fluorescein conjugated goat α-rabbit IgG F(AB') (i) and anti-β-actin and Alexa Fluor 546 α-mouse IgG_1 (ii) and visualized using confocal microscopy, with images taken of an identical field of view in different colour channels. These images were merged to generate the composite image, showing co-localisation of hShrm1 and β-actin (iii).

Interestingly, genes homologous to hShrm1 have been identified in a range of other species, including chimpanzee (98% similar to hShrm1 across the length of the protein), cow (70%) and mouse (61%) (Clustal W)[38]. Such conservation between species suggests that hShrm1 plays an important role within the cell. Two splice variants of hShrm1 have also been described that differ by 5 amino acids within the ASD2 domain. Variant 1 is a 752 amino acid protein and is considered the canonical sequence (UniProtKB entry Q2M3G4) whereas variant 2, the isoform identified in this study, has a 5-residue deletion (ASLLQ) following amino acid 742 [39, 40]. The significance of this insertion/deletion is not known.

RT-PCR analysis indicates hShrm1 is expressed in a range of tissues including brain, skeletal muscle, small intestine, kidney, lung and thymus (Fig. 5B). This is similar to the hShrm1 microarray expression data published on the UCSC Genome Browser [33], which identifies liver and prostate as expressing the highest relative amounts of hShrm1, followed by heart, muscle, spleen and testes. In our experiments, hShrm1 expression also appeared to be high in some tumour tissues and melanoma cell lines (Fig. 5A). As we had originally identified hShrm1 as a binding partner of MCAM-L the possibility that mShrm1 and MCAM expression levels were positively correlated was investigated. However, no association was found between the mRNA levels of hShrm1 and MCAM cell surface protein levels in the melanoma cells tested. Furthermore, MCAM positive melanoma cells and MCAM negative keratinocytes expressed similar amounts of hShrm1 mRNA (Fig. 5C). Taken together, these data suggest that hShrm1 expression is independent of MCAM expression and that hShrm1 is likely to play a broader role within the cell than simply as a binding partner of MCAM.

This conclusion was supported by the *in vivo* work in mammalian cells. In the co-immunoprecipitation experiments, the α-hShrm1 anti-serum pulled down only a small amount of MCAM relative to the MCAM immunoprecipitated by the α-MCAM antibody (Fig. 6D). In addition, although the BRET ratios were statistically significant and consistent, they were relatively small, indicating a modest interaction between hShrm1 and MCAM (Fig. 8A). Lastly, only a proportion of the intracellular pools of hShrm1 and MCAM co-localise within the cell, primarily in the peri-nuclear region (Fig. 7). The specific identity of the intracellular compartments in which hShrm1 and MCAM co-localise requires further investigation. Although we were able to demonstrate MCAM

A.

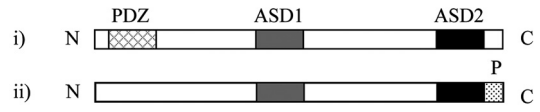

B.

GenBank Accession Number	Historical name	Organism	New name
CAA78718	Apx	X. laevis	xShroom1
NP_597713	ApxL2	H. sapiens	hShroom1
ABD19518	ApxL	M. musculus	mShroom2
CAA58534	ApxL	H. sapiens	hShroom2
ABD59319	Shroom-like	X. laevis	xShroom3
AAF13269	ShroomL	M. musculus	mShroom3a
AF13270	ShroomS	M. musculus	mShroom3b
NP_065910	Shroom	H. sapiens	hShroom3
DQ435686	KIAA1202	M. musculus	mShroom4
NP_065768	KIAA1202	H. sapiens	hShroom4a
AAK95579	SHAP-A	H. sapiens	hShroom4b

Figure 10. The Shrm protein family. (*A*) A typical example of a Shrm family protein is shown in (i) and hShrm1 in (ii). The Shrm family is defined by the presence of an N-terminal PDZ domain (hatched box), a central ASD1 motif (grey box) and a C-terminal ASD2 motif (black box). hShrm1 contains a C-terminal proline-rich region not present in other Shrm proteins but does not have the PDZ domain. (*B*) The standard nomenclature and sub-families of the Shrm proteins

localisation in the golgi apparatus, we found no evidence of such localisation of hShrm1 (data not shown).

There is some evidence that MCAM may associate with recycling endosomes, which is consistent with a perinuclear localisation. In an elegant study investigating the effect of Wnt5a expression on the cellular distribution of MCAM, Witze et al. (2008) [41] found that MCAM partially co-localises with Rab4 (a marker of early endosomes) and that Wnt5a-driven intracellular translocation of MCAM was dependent upon internalisation of MCAM and the trafficking of receptor endosomes [41]. Experiments performed in our laboratory indicate that MCAM is rapidly and constitutively recycled from the cell surface and the data are consistent with the suggestion that MCAM movement through the cell involves recycling endosomes (unpublished observations). Thus, it is possible that hShrm1 may be localising on the cytoplasmic face of recycling endosomes and interacting with MCAM at this site.

We next investigated which region of hShrm1 was responsible for binding to MCAM. The original hShrm1 clone (2H-clone7) (Fig. 4) that bound to MCAM in the yeast two-hybrid experiments contained the C-terminal half of hShrm1, starting at amino acid 481 (reference sequence: UniProtKB entry Q2M3G4) [39]. However, BRET analysis indicated that hShrm1 fusion proteins lacking both the proline-rich and ASD2 motifs bound the MCAM cytoplasmic tail to the same degree as full-length hShrm1, suggesting that these regions are not essential for the hShrm1-MCAM interaction (Fig. 8b). Thus, the MCAM-binding region of hShrm1 is likely to fall between amino acids 481 and 543 (the start of the ASD2 domain). Interestingly, no binding properties or putative functions have been attributed to the region between ASD1 and ASD2 in other Shrm family members.

The region of MCAM responsible for binding to hShrm1 was also investigated. BRET analysis revealed that hShrm1 binds to the cytoplasmic tail of MCAM in a region proximal to the transmembrane domain (Figs. 1 and 8a). Interestingly, there is evidence that gicerin, the chicken homologue of MCAM, contains a moesin binding site in this membrane-proximal region [42]. As the intracellular domains of MCAM and gicerin are highly homologous [13], MCAM may also interact with moesin or another ERM (ezrin-radixin-moesin) protein at this membrane proximal site. The ERM proteins act as a link between plasma membrane proteins and the cortical cytoskeleton and are therefore involved in regulating some of the fundamental functions of membrane bound proteins, such as cell shape determination, cell adhesion and cell motility [43]. Further investigation is required to investigate whether ERM proteins also bind to MCAM, if ERM proteins and hShrm1 compete for this binding site, and if other Shrm family members also bind MCAM.

Given that the interaction between hShrm1 and MCAM probably involves only a small proportion of intracellular hShrm1, it is possible that this protein links the cellular cytoskeleton to a number of as-yet-unknown membrane-associated proteins. The only other Shrm protein that has been associated with a membrane protein is xShrm1. xShrm1 was identified as part of a apical membrane macromolecular protein complex associated with the amiloride-sensitive epithelial sodium channel (ENaC) [4, 5, 44, 45]. Staub and co-workers found that xShrm1 was necessary but not sufficient for the activity of amiloride-sensitive sodium currents in *Xenopus* oocytes, and suggested that hShrm1 may play a regulatory role [4]. Zuckerman et al. [5] confirmed these findings and proposed that xShrm1 was required for functional expression of ENaC in *Xenopus* A6 renal epithelial cells. In addition, the protein complex containing ENaC and xShrm1 was also found to contain spectrin, a cytoske-

letal protein that combines with short actin filaments to form a supportive scaffold on the intracellular aspect of plasma membranes of many cells [46]. The association of ENaC with xShrm1 and the spectrin-based membrane cytoskeleton may act to sequester and stabilize ENaC within micro-domains of the apical plasma membrane, and so contribute to the regulation of ENaC activity [5]. Another group reported that ENaC activity was regulated by both xShrm1 and the actin cytoskeleton [47, 48], which is broadly supportive of the "sequester and stabilise" model described above.

Although there are some similarities between our data and that reported for xShrm1 (e.g. both hShrm1 and xShrm1 display large intracellular pools, and both MCAM and ENaC were only weakly detected in hShrm1/xShrm1 precipitates), an important difference is the subcellular location. The hShrm1-MCAM interaction detected in this study appears to occur primarily within intracellular compartments, whereas the xShrm1-ENaC complex is located at the apical plasma membrane.

The Shrm protein family influences diverse cellular processes such as morphogenesis [7–9], retinal epithelial pigmentation [3] and neural development [11], with the common theme being the regulation of cellular architecture [2]. The conserved ASD1 and ASD2 motifs appear to play a significant role in this. The ASD2 domain is capable of regulating cell shape via actin, myosin and/or γ-tubulin accumulation within the cell [10]. However, the ability of myosin and/or γ-tubulin to cause cell shape changes such as apical constriction and apicobasal elongation is modulated by the actin-binding properties and subsequent disparate cellular localisation of the Shrm proteins. Shrm2 binds to cortical actin whereas Shrm3 binds to and bundles F-actin stress-fibres [7, 8, 37]. Interestingly, the ASD1 domain alone is sufficient for subcellular localisation of Shrm3, whereas both ASD1 and the PDZ domains are necessary for optimal targeting of Shrm2 [37]. In contrast, Shrm4 lacks an ASD1 motif, but the central portion of the protein, although sharing no homology to other actin-binding motifs, appears to regulate the cytoskeletal location of Shrm4. Shrm4 is found either at the apical plasma membrane or associated with a punctate/filamentous cytoplasmic structure, both of which are coincident with F-actin [2].

In conclusion, our data represent the first characterisation of hShrm1, which we suggest may represent a new subfamily of Shrm proteins. We identified hShrm1 opportunistically from a yeast two hybrid screen using the intracellular tail of MCAM as bait. hShrm1 is expressed in a range of tissues and cell lines, and evidence confirming the interaction between hShrm1 and MCAM in mammalian cells was obtained from co-immunoprecipitation, confocal microscopy and BRET experiments. hShrm was also found to partially co-localise with the actin cytoskeleton. In melanoma cells, the data suggest that hShrm1 may be involved in linking MCAM to the actin cytoskeleton. However, hShrm1 exists in a sizable intracellular pool, only some of which interacts with MCAM, suggesting that hShrm1 is likely to interact with a number of other proteins.

Acknowledgements. We thank J. Mirkovitch and E. Seger for excellent technical help and R. Seeber for her assistance with the BRET analysis. We are most grateful to Dr. B. Giovanella for the gift of the SB1 and SB2 cell lines. This work was supported by a grant from the Bernese Cancer League to S.K. and in part by a grant to D.R.C. from the Raine Foundation and the Cancer Foundation of Western Australia.

1 Hagens, O., Ballabio, A., Kalscheuer, V., Kraehenbuhl, J. P., Schiaffino, M. V., Smith, P., Staub, O., Hildebrand, J. and Wallingford, J. B. (2006) A new standard nomenclature for proteins related to Apx and Shroom. BMC Cell. Biol. 7, 18.
2 Yoder, M. and Hildebrand, J. D. (2007) Shroom4 (Kiaa1202) is an actin-associated protein implicated in cytoskeletal organization. Cell Motil. Cytoskeleton 64, 49–63.
3 Fairbank, P. D., Lee, C., Ellis, A., Hildebrand, J. D., Gross, J. M. and Wallingford, J.B. (2006) Shroom2 (APXL) regulates melanosome biogenesis and localization in the retinal pigment epithelium. Development 133, 4109–18.
4 Staub, O., Verrey, F., Kleyman, T. R., Benos, D. J., Rossier, B. C. and Kraehenbuhl, J.P. (1992) Primary structure of an apical protein from Xenopus laevis that participates in amiloride-sensitive sodium channel activity. J. Cell Biol. 119, 1497–506.
5 Zuckerman, J. B., Chen, X., Jacobs, J. D., Hu, B., Kleyman, T. R. and Smith, P. R. (1999) Association of the epithelial sodium channel with Apx and alpha-spectrin in A6 renal epithelial cells. J. Biol. Chem. 274, 23286–95.
6 Schiaffino, M. V., Bassi, M. T., Rugarli, E. I., Renieri, A., Galli, L. and Ballabio, A. (1995) Cloning of a human homologue of the Xenopus laevis APX gene from the ocular albinism type 1 critical region. Hum. Mol. Genet. 4, 373–82.
7 Haigo, S. L., Hildebrand, J. D., Harland, R. M. and Wallingford, J. B. (2003) Shroom induces apical constriction and is required for hingepoint formation during neural tube closure. Curr. Biol. 13, 2125–37.
8 Hildebrand, J. D. and Soriano, P. (1999) Shroom, a PDZ domain-containing actin-binding protein, is required for neural tube morphogenesis in mice. Cell 99, 485–97.
9 Hildebrand, J. D. (2005) Shroom regulates epithelial cell shape via the apical positioning of an actomyosin network. J. Cell Sci. 118, 5191–203.
10 Lee, C., Scherr, H. M. and Wallingford, J.B. (2007) Shroom family proteins regulate gamma-tubulin distribution and microtubule architecture during epithelial cell shape change. Development 134, 1431–41.
11 Hagens, O., Dubos, A., Abidi, F., Barbi, G., Van Zutven, L., Hoeltzenbein, M., Tommerup, N., Moraine, C., Fryns, J. P., Chelly, J., van Bokhoven, H., Gecz, J., Dollfus, H., Ropers, H. H., Schwartz, C. E., de Cassia Stocco Dos Santos, R., Kalscheuer, V. and Hanauer, A. (2006) Disruptions of the novel KIAA1202 gene are associated with X-linked mental retardation. Hum. Genet. 118, 578–90.
12 Lehmann, J. M., Riethmuller, G. and Johnson, J. P. (1989) MUC18, a marker of tumor progression in human melanoma, shows sequence similarity to the neural cell adhesion molecules

of the immunoglobulin superfamily. Proc. Natl Acad. Sci. USA 86, 9891–5.
13 Alais, S., Allioli, N., Pujades, C., Duband, J. L., Vainio, O., Imhof, B. A. and Dunon, D. (2001) HEMCAM/CD146 down-regulates cell surface expression of (beta) 1 integrins. J. Cell Sci. 114, 1847–59.
14 Johnson, J. P., Bar-Eli, M., Jansen, B. and Markhof, E. (1997) Melanoma progression-associated glycoprotein MCU18/MCAM mediates homotypic cell adhesion through interaction with a heterophilic ligand. Int. J. Cancer 73, 769–74.
15 Shih, I. M., Speicher, D., Hsu, M. Y., Levine, E. and Herlyn, M. (1997) Melanoma cell-cell interactions are mediated through heterophilic Mel-CAM/ligand adhesion. Cancer Res. 57, 3835–40.
16 Anfosso, F., Bardin, N., Frances, V., Vivier, E., Camoin-Jau, L., Sampol, J. and Dignat-George, F. (1998) Activation of human endothelial cells via S-endo-1 antigen (CD146) stimulates the tyrosine phosphorylation of focal adhesion kinase p125(FAK). J. Biol. Chem. 273, 26852–6.
17 Anfosso, F., Bardin, N., Vivier, E., Sabatier, F., Sampol, J. and Dignat-George, F. (2001) Outside-in signaling pathway linked to CD146 engagement in human endothelial cells. J. Biol.-Chem. 276, 1564–9.
18 Marin, V., Kaplanski, G., Gres, S., Farnarier, C. and Bongrand, P. (2001) Endothelial cell culture: protocol to obtain and cultivate human umbilical endothelial cells. J Immunol. Methods 254, 183–90.
19 Karlen, S. and Braathen, L. R. (1999) Regulation of the melanoma cell adhesion molecule gene in melanoma: modulation of mRNA synthesis by cyclic adenosine monophosphate, phorbol ester, and stem cell fFactor/c-kKit signaling. J. Invest. Dermatol. 11, 711–9.
20 Durfee, T., Becherer, K., Chen, P. L., Yeh, S. H., Yang, Y., Kilburn, A. E., Lee, W. H. and Elledge, S. J. (1993) The retinoblastoma protein associates with the protein phosphatase type 1 catalytic subunit. Genes Dev. 7, 555–69.
21 Schiestl, R. H. and Gietz, R. D. (1989) High efficiency transformation of intact yeast cells using single stranded nucleic acids as a carrier. Curr. Genet. 16, 339–46.
22 Breeden, L. and Nasmyth, K. (1985) Regulation of the yeast HO gene. Cold Spring Harb. Symp. Quant. Biol. 50, 643–50.
23 Staub, O., Dho, S., Henry, P., Correa, J., Ishikawa, T., McGlade, J. and Rotin, D. (1996) WW domains of Nedd4 bind to the proline-rich PY motifs in the epithelial Na+ channel deleted in Liddle's syndrome. EMBO J. 15, 2371–80.
24 Guarente, L. (1983) Yeast promoters and lacZ fusions designed to study expression of cloned genes in yeast. Methods Enzymol. 101, 181–91.
25 Miller, J. H. (1972) Experiments in Molecular Genetics. Cold Spring Harbor Laboratory Press, Cold Spring Harbor, NY.
26 Filshie, R. J., Zannettino, A. C., Makrynikola, V., Gronthos, S., Henniker, A. J., Bendall, L. J., Gottlieb, D. J., Simmons, P. J. and Bradstock, K. F. (1998) MUC18, a member of the immunoglobulin superfamily, is expressed on bone marrow fibroblasts and a subset of hematological malignancies. Leukemia 12, 414–21.
27 Kroeger, K. M., Hanyaloglu, A. C., Seeber, R. M., Miles, L. E. and Eidne, K. A. (2001) Constitutive and agonist-dependent homo-oligomerization of the thyrotropin-releasing hormone receptor. Detection in living cells using bioluminescence resonance energy transfer. J. Biol. Chem. 276, 12736–43.
28 Eidne, K. A., Kroeger, K. M. and Hanyaloglu, A. C. (2002) Applications of novel resonance energy transfer techniques to study dynamic hormone receptor interactions in living cells. Trends Endocrinol. Metab. 13, 415–21.
29 Sers, C., Kirsch, K., Rothbacher, U., Riethmuller, G. and Johnson, J.P. (1993) Genomic organization of the melanoma-associated glycoprotein MUC18: implications for the evolution of the immunoglobulin domains. Proc. Natl Acad. Sci. USA 90, 8514–8.
30 Marks, M. S., Woodruff, L., Ohno, H. and Bonifacino, J. S. (1996) Protein targeting by tyrosine- and di-leucine-based signals: evidence for distinct saturable components. J. Cell Biol. 135, 341–54.
31 Kozak, M. (1989) The scanning model for translation: an update. J. Cell Biol. 108, 229–41.
32 Kent, W. J. (2002) BLAT–the BLAST-like alignment tool. Genome Res 12, 656–64.
33 Karolchik, D., Baertsch, R., Diekhans, M., Furey, T. S., Hinrichs, A., Lu, Y. T., Roskin, K. M., Schwartz, M., Sugnet, C. W., Thomas, D. J., Weber, R. J., Haussler, D. and Kent, W. J. (2003) The UCSC Genome Browser Database. Nucl. Acids Res. 31, 51–4.
34 Pruitt, K. D., Tatusova, T. and Maglott, D. R. (2005) NCBI Reference Sequence (RefSeq): a curated non-redundant sequence database of genomes, transcripts and proteins. Nucl. Acids Res. 33, D501–4.
35 Bardin, N., Anfosso, F., Masse, J. M., Cramer, E., Sabatier, F., Le Bivic, A., Sampol, J. and Dignat-George, F. (2001) Identification of CD146 as a component of the endothelial junction involved in the control of cell-cell cohesion. Blood 98, 3677–84.
36 Shih, I. M. (1999) The role of CD146 (Mel-CAM) in biology and pathology. J. Pathol. 189, 4–11.
37 Dietz, M. L., Bernaciak, T. M., Vendetti, F., Kielec, J. M. and Hildebrand, J. D. (2006) Differential actin-dependent localization modulates the evolutionarily conserved activity of Shroom family proteins. J. Biol. Chem. 281, 20542–54.
38 Larkin, M. A., Blackshields, G., Brown, N. P., Chenna, R., McGettigan, P. A., McWilliam, H., Valentin, F., Wallace, I. M., Wilm, A., Lopez, R., Thompson, J. D., Gibson, T. J. and Higgins, D. G. (2007) Clustal W and Clustal X version 2.0. Bioinformatics 23, 2947–8.
39 The UniProt Consortium. (2008) The Universal Protein Resource (UniProt). Nucl. Acids Res. 36, D190–5.
40 Nagase, T., Kikuno, R. and Ohara, O. (2001) Prediction of the coding sequences of unidentified human genes. XXII. The complete sequences of 50 new cDNA clones which code for large proteins. DNA Res. 8, 319–27.
41 Witze, E. S., Litman, E. S., Argast, G. M., Moon, R. T. and Ahn, N. G. (2008) Wnt5a control of cell polarity and directional movement by polarized redistribution of adhesion receptors. Science 320, 365–9.
42 Okumura, S., Muraoka, O., Tsukamoto, Y., Tanaka, H., Kohama, K., Miki, N. and Taira, E. (2001) Involvement of gicerin in the extension of microvilli. Exp. Cell Res. 271, 269–76.
43 Bretscher, A., Edwards, K. and Fehon, R. G. (2002) ERM proteins and merlin: integrators at the cell cortex. Nat. Rev. Mol. Cell Biol. 3, 586–99.
44 Benos, D. J., Saccomani, G. and Sariban-Sohraby, S. (1987) The epithelial sodium channel. Subunit number and location of the amiloride binding site. J. Biol. Chem. 262, 10613–8.
45 Kleyman, T. R., Kraehenbuhl, J. P. and Ernst, S. A. (1991) Characterization and cellular localization of the epithelial Na+ channel. Studies using an anti-Na+ channel antibody raised by an antiidiotypic route. J. Biol. Chem. 266, 3907–15.
46 Bennett, V. and Healy, J. (2008) Organizing the fluid membrane bilayer: diseases linked to spectrin and ankyrin. Trends Mol. Med.14, 28–36.
47 Cantiello, H. F., Stow, J. L., Prat, A. G. and Ausiello, D. A. (1991) Actin filaments regulate epithelial Na+ channel activity. Am. J. Physiol. 261, C882–8.
48 Prat, A. G., Holtzman, E. J., Brown, D., Cunningham, C. C., Reisin, I. L., Kleyman, T. R., McLaughlin, M., Jackson, G. R., Jr., Lydon, J. and Cantiello, H. F. (1996) Renal Epithelial Protein (Apx) Is an Actin Cytoskeleton-regulated Na+ Channel. J. Biol. Chem. 271, 18045–53.